Open Access Journal
Journal of Power Technologies 91 (4) (2011) 179–185
journal homepage:papers.itc.pw.edu.pl

The influence of fuel composition on Solid Oxide Fuel Cell obtained by using the advanced mathematical model

Jarosław Milewski*

Institute of Heat Engineering, Warsaw University of Technology
21/25 Nowowiejska Street, 00-665 Warsaw, Poland

Abstract

The advanced mathematical model of Solid Oxide Fuel Cell (SOFC) is presented. The governing equations of the model are presented and described. Based on the model the influence of fuel composition on SOFC performance is shown. Hydrogen is used as the reference fuel.

Keywords: fuel cell, Solid Oxide Fuel Cell, mathematical modelling

1. Introduction

Fuel cells are very promising technology for power generation in the future due to the direct conversion of fuel into electricity. Fuel cell units are relatively small [1]. High temperature fuel cells (mainly SOFC and Molten Carbonate Fuel Cell – MCFC) can be coupled with other devices like gas turbines [2–7] (making a hybrid system) or even used in polygeneration [8].

There are many mathematical models of the singular solid oxide fuel cell (SOFC) [9–12]. SOFC performance modelling is related to the multi-physic processes taking place on the fuel cell surfaces [13–15]. Heat transfer together with electrochemical reactions, mass [15] and charge transport are conducted inside the cell. The SOFC models found in the literature are based mainly on mathematical descriptions of these physical, chemical, and electrochemical properties.

The SOFC models developed thus far are mainly based on the Nernst equation, activation, ohmic, and concentration losses. Actually, this means that the specific current-voltage curve is approximated by several factors such as current limiting, exchange current and so forth. This approach results in good agreement with particular experimental data (for which adequate factors were obtained) and poor agreement for non-original experimental working parameters.

Moreover, most of the equations require the addition of numerous factors (porosity, tortuosity, ionic and electronic paths, etc.) which are difficult to determine and which are often related to the microscopic properties of the cell which govern both chemical and electrochemical reactions.

Those parameters are frequently used as fitting parameters without any physical background. This is particularly relevant in the case of complex fuel feeding. It is far from straightforward to determine all requisite coefficients and factors even for small number of current-voltage curves for hydrogen as a fuel only. Introduction of other components makes this task substantially more difficult. A new model is pro-

*Corresponding author
Email address: milewski@itc.pw.edu.pl (Jarosław Milewski*)

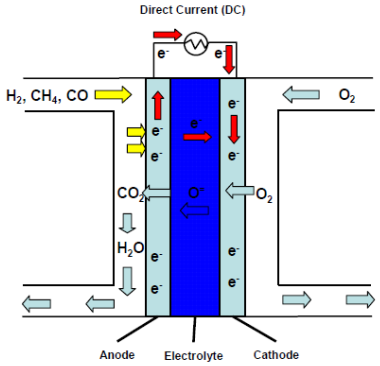

Figure 1: Working principles of SOFC

Table 1: Maximum voltages for various reactions

Chemical Reaction	Maximum Voltage, E_{max}, V at 20°C
$H_2+\frac{1}{2}O_2 \rightarrow H_2O$	1.23
$CH_4+2O_2 \rightarrow CO_2+H_2O$	1.06
$CH_3OH+\frac{3}{2}O_2 \rightarrow CO_2+2H_2O$	1.22
$C+O_2 \rightarrow CO_2$	1.03
$C+\frac{1}{2}O_2 \rightarrow CO$	0.72
$CO+\frac{1}{2}O_2 \rightarrow CO_2$	1.34

posed and the governing equations of this model are presented in this paper.

Because of the complexity of the models, fully empirical approaches can found in the literature [9, 16–23] to obtain reliable results during optimization and dynamic simulations.

2. Mathematical model of SOFC

Mathematical modelling is now the basic method for analyzing systems incorporating fuel cells. A zero-dimensional approach is used for the modelling of system elements.

2.1. Fuel cell voltage

The working principles of SOFC are shown in Fig. 1. The oxygen partial pressure difference between anode and cathode forces oxygen ions ($O^=$) to pass through the solid electrolyte. This process generates voltage and an electric current can be drawn from the cell.

The maximum voltage of the fuel cell depends on the type of reaction occurring on the electrode surfaces. The maximum voltages for various reactions are listed in Table 1. It can be seen that various fuels in reaction with oxygen can give various maximum voltages. Mixtures of various components occur in the case of the analyzed fuels. Due to these circumstances the general form of Nernst's equation is used to estimate the voltage of SOFC:

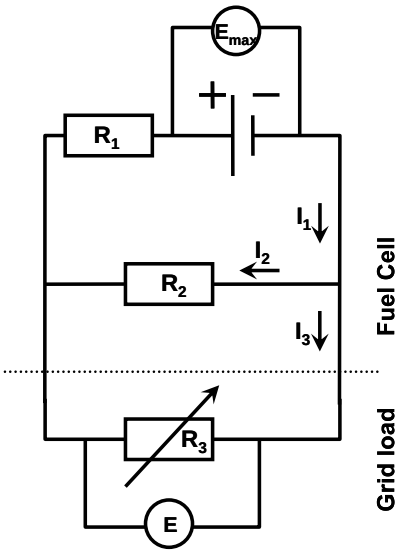

Figure 2: Equivalent electric circuit of the cell

$$E_{\max} = \frac{R \cdot T}{4F} \ln \frac{p_{O_2,cathode}}{p_{O_2,anode}} \tag{1}$$

Adequate partial pressures can be calculated based on the thermodynamic functions of the Peng-Robinson equation of state and minimization of Gibbs free energy [24].

The equivalent electric circuit of a singular cell is shown in Fig. 2. The total current which can be drawn from the cell is strictly correlated with the amount of fuel delivered. This means that it is a value of current for which the whole fuel is utilized – $I_{\max}$. Then, the fuel utilization factor can be correlated with the current generated by the cell:

$$I_3 = (I_{\max} - I_2) \cdot \eta_f \tag{2}$$

$$I_{\max} = 2F \cdot \dot{n}_{H_2,equivalent} \tag{3}$$

The mixture of various fuels enters into the SOFC anode, so the fuel utilization factor is calculated based on an equivalent hydrogen molar flow, which is defined by the following relationship:

$$\begin{aligned}\dot{n}_{H_2,equivalent} = {} & \dot{n}_{H_2} + \dot{n}_{CO} \\ & + 3 \cdot \dot{n}_{CH_3OH} + 4 \cdot \dot{n}_{CH_4} \\ & + 6 \cdot \dot{n}_{C_2H_3OH} + 7 \cdot \dot{n}_{C_2H_6} \\ & + 10 \cdot \dot{n}_{C_3H_8} + 13 \cdot \dot{n}_{C_4H_{10}}\end{aligned} \quad (4)$$

Two types of resistance are present in fuel cells: ionic resistance r_1 and electric resistance r_2 (see Fig. 2). Resistance r_3 is the external load resistance of the fuel cell. The second resistance has meaning of electrons passing through the electrolyte layer. For the electric circuit shown in Fig. 2, using Ohm's and Kirchhoff's laws, a set of equations can be built as follows:

$$\begin{cases} E_{\max} = r_1 \cdot i_1 + r_2 \cdot i_2 \\ i_1 = i_2 + i_3 \\ E_{SOFC} = r_2 \cdot i_2 \end{cases} \quad (5)$$

By solving both the set of Equations 5 and Equation 2 an equation for the cell voltage is obtained [25]:

$$E_{SOFC} = \frac{E_{\max} - i_{max} \cdot \eta_f \cdot r_1}{\frac{r_1}{r_2} \cdot \left(1 - \eta_f\right) + 1} \quad (6)$$

The value of maximum current density ($i_{\max}$) is constant in the design point calculations. In the case of design point calculations, the voltage-fuel utilization factor curve ($E = f\left(\eta_f\right)$) is the fuel cell characteristic. E.g. the $i_{\max}$ of 4.58A/cm^2 was determined by the researchers' own calculations, which were based on data taken from [26, 27]. This means that in design point calculations the cell area is always fixed in relation to inlet fuel flow. A lower value of the $i_{\max}$ means a larger cell area of the fuel cell for the same fuel utilization factor.

The fuel cell characteristic is defined by a voltage-current density curve ($E = f(i)$). The area of the cell is fixed during off-design calculations, which means that factor $i_{\max}$ has to be calculated based on the following equations:

$$i_{\max} = \frac{2 \cdot F \cdot n_{H_2,equivalent}}{A} \quad (7)$$

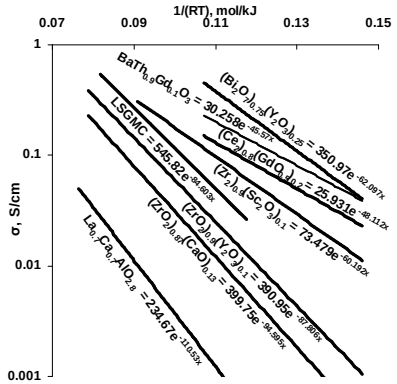

Figure 3: Temperature dependence of ionic conductivity for solid oxides

2.2. Area specific ionic resistance

Total ionic resistance of the cell is a function of many parameters. The solid oxide fuel cell consists of electrolyte covered by anode and cathode layers. Those layers influence ionic conductivity as well (e.g. triple boundary phase processes). The material used, porosity and design of the electrodes have a significant influence on fuel cell voltage.

$$r_{1,total} = \sum \frac{\delta_{electrolyte}}{\sigma_{electrolyte}} + \sum \frac{\delta_{anode}}{\sigma_{anode}} + \sum \frac{\delta_{cathode}}{\sigma_{cathode}} \quad (8)$$

The ionic conductivity of the solid oxide is defined as follows:

$$\sigma = \sigma_0 \cdot e^{\frac{-E_\sigma}{R \cdot T}} \quad (9)$$

The ionic resistance of solid oxides as a function of electrolyte temperature is shown in Fig. 4.

2.3. Area specific electric specific resistance

In general, solid oxides are assumed to be only ionic conductors, but in fact electron conductivity is present as well [28]. Gas leakage through the electrolyte has the same effect as electron (electrical) conductance and can be described in the same way.

The second type of internal resistance is electrical resistance – r_2 (see Fig. 2). The influences of temperature and electrolyte thickness on electronic internal resistance of electrolytes are not well known. The electronic conductivity values of solid oxide electrolytes are probably spread across a very wide range [29]. They do not have a major impact on

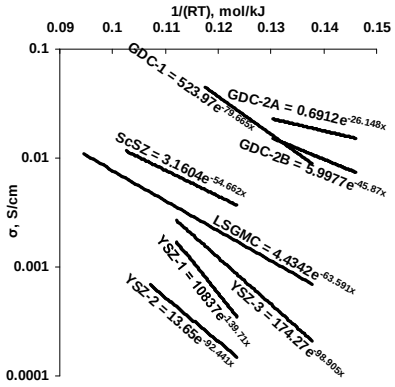

Figure 4: Temperature dependence of electrical conductivity for solid oxides

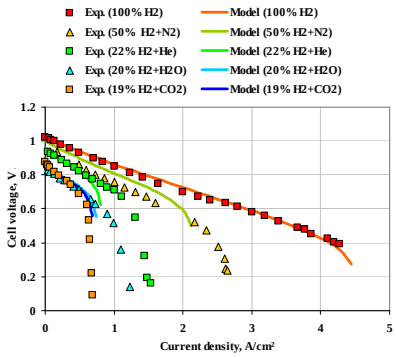

Figure 5: Experimental and simulation data at various fuel compositions for experimental data taken from [26]. Temperature 800°C, air as oxidant

calculated cell voltage for high fuel utilization factors. It is difficult to measure the electronic resistance of solid oxide electrolytes since they have both conductivities – ionic and electronic – simultaneously, which gives total electrical resistance. It should be noted that decreasing electrolyte thickness reduces ionic resistance, but also probably reduces electronic resistance.

Apart from a physical explanation of the difference between calculated maximum cell voltage and related open circuit voltage, for given r_1, $E_{\max}$ and E_{OCV} (from experimental measurements) the value of electrical resistance of the cell can be found by using the following relationship:

$$r_2 = \frac{\delta}{\sigma_2} \tag{10}$$

The value of electrical resistance of the cell can be estimated from available experimental results. Substituting $\eta_f = 0$ into Eq. 6, the E_{OCV} can be defined by the following relationship:

$$E_{OCV} = \frac{E_{\max}}{\frac{r_1}{r_2} + 1} \tag{11}$$

Substituting Eq. 10 into Eq. 11, the relationship for electrical conductivity of the cell is obtained:

$$\sigma_2 = \delta \cdot \frac{E_{\max} - E_{OCV}}{r_1 \cdot E_{OCV}} \tag{12}$$

The electrical conductivities of solid oxides were estimated by using Eq. 12 and based on experimental data published in [30–37]. The result of this estimation is shown in Fig. 4.

3. Model validation

The presented model was compared with experimental data [26]; this comparison is shown in Fig. 5. The tested cell has a diameter of 2.6 cm, and the following oxidant and fuel flows were kept constant: oxidant 550 Nml/min and fuel 140 Nml/min, respectively. The cell was tested at a constant temperature of 800°C.

The tested cell was constructed of YSZ-SDC bilayer electrolyte supported by the anode layer. The thickness of the SDC layer was around 3 μm and the total thickness of the YSZ-SDC bilayer electrolyte thin film was 10 μm. Then, the ionic resistance of the fuel cell was calculated as follows:

$$r_1 = \frac{\delta_{SDC}}{\sigma_{SDC}} + \frac{\delta_{YSZ}}{\sigma_{YSZ}} + r_{electrodes} \tag{13}$$

Adequate factors of ionic conductivity for both layers were read from Fig. 3, whereas resistance of the electrodes was fitted (in fact there is only one fitting parameter in the model) and assumed constant: 0.06 cm²/S. It should be noted that electrode losses are significant (62%) at 800°C compared with electrolyte losses. Often, both anode and cathode layers contain the same material which is used for electrolyte. It is evident that temperature has a significant influence. Further work will focus on finding adequate relationships for that.

Voltages and current densities were calculated based on equations presented in this paper. The model was compared with experimental data for hydrogen as a fuel diluted by helium and hydrogen as a

fuel diluted with steam; this comparison is shown in Fig. 5.

4. Discussion

SOFC fuelled by dry hydrogen is modelled with higher accuracy than other fuel compositions. While lower hydrogen content in the fuel mixture is modelled with a higher degree of error, on the other hand the shapes of the obtained curves generally follow the experimental data.

The OCVs given by the model are almost the same as the experimental data. Significant differences occur with low hydrogen content; this affects situations where hydrogen is diluted with helium and steam.

The crucial issue in fuel cell voltage estimation is calculating the Nernst voltage using Eq. 1. Firstly, oxygen partial pressures should be calculated at the outlet streams. Secondly, chemical equilibrium is assumed at the anode, which is mainly true in the case of hydrogen as a fuel. For other fuels, adequate kinetic calculations must be proceeded to obtain an accurate value of oxygen partial pressure [38]. Additionally, the presence of any catalytic medium [39] can impact the manner of obtaining accurate results.

5. Conclusions

The advanced mathematical model of SOFC is presented. The governing equations of the model are presented and described. Based on the model the influence of fuel composition on SOFC performance is shown. Hydrogen is used as the reference fuel.

The proposed model gives acceptable results for various fuel compositions. Simultaneously, dry hydrogen as well as hydrogen diluted with other components (He, H_2O, CO_2, N_2) is modelled with a relatively small degree of error. The proposed model gives physical results for the whole range of parameters. Assuming the fuel utilization factor as zero, the equation for open circuit voltage is obtained. The difference between the $E_{\max}$ and E_{OCV} is expressed.

References

[1] A. Lanzini, M. Santarelli, G. Orsello, Residential solid oxide fuel cell generator fuelled by ethanol: Cell, stack and system modelling with a preliminary experiment, Fuel Cells 10 (4) (2010) 654–675.

[2] F. Mueller, R. Gaynor, A. Auld, J. Brouwer, F. Jabbari, G. G.S. Samuelsen, Synergistic integration of a gas turbine and solid oxide fuel cell for improved transient capability, Journal of Power Sources 176 (1) (2008) 229–239.

[3] K. Colombo, V. Kharton, O. Bolland, Simulation of an oxygen membrane-based gas turbine power plant: Dynamic regimes with operational and material constraints, Energy and Fuels 24 (1) (2010) 590–608.

[4] B. Tarroja, F. Mueller, J. Maclay, J. Brouwer, Parametric thermodynamic analysis of a solid oxide fuel cell gas turbine system design space, Journal of Engineering for Gas Turbines and Power 132 (7) (2010) 072301.

[5] J.-H. Wee, Molten carbonate fuel cell and gas turbine hybrid systems as distributed energy resources, Applied Energy doi:10.1016/j.apenergy.2011.05.043 (2011) Article in Press.

[6] W. Wu, J.-J. Luo, Nonlinear feedback control of a preheater-integrated molten carbonate fuel cell system, Journal of Process Control 20 (7) (2010) 860–868.

[7] L. G. C. J. Zhang, H., Performance analysis and multiobjective optimization of a new molten carbonate fuel cell system, International Journal of Hydrogen Energy 36 (6) (2011) 4015–4021.

[8] F. Al-Sulaiman, I. Dincer, F. Hamdullahpur, Energy analysis of a trigeneration plant based on solid oxide fuel cell and organic rankine cycle, International Journal of Hydrogen Energy 35 (10) (2010) 5104–5113.

[9] J. Milewski, K. Świrski, M. Santarelli, P. Leone, Advanced Methods of Solid Oxide Fuel Cell Modeling, 1st Edition, Springer-Verlag London Ltd., 2011.

[10] S. Kakac, A. Pramuanjaroenkij, X. Zhou, A review of numerical modeling of solid oxide fuel cells, International Journal of Hydrogen Energy 32 (7) (2007) 761–786.

[11] S. Hajimolana, M. Hussain, W. Daud, M. Soroush, A. Shamiri, Mathematical modeling of solid oxide fuel cells: A review, Renewable and Sustainable Energy Reviews 15 (4) (2011) 1893–1917.

[12] K. Wang, D. Hissel, M. Pera, N. Steiner, D. Marra, M. Sorrentino, C. Pianese, M. Monteverde, P. Cardone, J. Saarinen, A review on solid oxide fuel cell models, International Journal of Hydrogen Energy 36 (12) (2011) 7212–7228.

[13] H. Cao, Z. Deng, X. Li, J. Yang, Y. Qin, Dynamic modeling of electrical characteristics of solid oxide fuel cells using fractional derivatives, International Journal of Hydrogen Energy 35 (4) (2010) 1749–1758.

[14] H. Cao, X. Li, Z. Deng, J. Jiang, J. Yang, J. Li, Y. Qin, Dynamic modeling and experimental validation for the electrical coupling in a 5-cell solid oxide fuel cell stack in the perspective of thermal coupling, International Journal of Hydrogen Energy 36 (7) (2011) 4409–4418.

[15] K. Christman, M. Jensen, Solid oxide fuel cell performance with cross-flow roughness, Journal of Fuel Cell Science and Technology 8 (2) (2011) 024501.

[16] N. Kishor, S. Mohanty, Fuzzy modeling of fuel cell based on mutual information between variables, International

Journal of Hydrogen Energy 35 (8) (2010) 3620–3631.
[17] N. Sisworahardjo, T. Yalcinoz, M. El-Sharkh, M. Alam, Neural network model of 100 w portable pem fuel cell and experimental verification, International Journal of Hydrogen Energy 35 (17) (2010) 9104–9109.
[18] J. Milewski, B. Deszczyński, K. Świrski, Artificial neural network as sofc model, in: Elsevier, Fuel Cells Science and Technology, no. 4, 2008, p. 1B.2.
[19] J. Milewski, M. Santarelli, K. Świrski, Modelling of solid oxide fuel cell behaviour by artificial neural network, in: Fundamentals and Development in Fuel Cells, Grenoble, France, 2008.
[20] J. Milewski, K. Świrski, M. Santarelli, P. Leone, Modelling of fuel composition influences on solid oxide fuel cell performance by artificial neural network, Archives of Thermodynamics 30 (4) (2009) 13–24.
[21] J. Milewski, K. Świrski, Modelling the SOFC behaviours by artificial neural network, International Journal of Hydrogen Energy 34 (13) (2009) 5546–5553.
[22] J. Milewski, K. Świrski, P. Leone, M. Santarelli, Modelling the influence of fuel composition on SOFC performance by artificial neural network, in: European Fuel Cell Technology & Applications – "Piero Lunghi Conference", no. EFC09-17007, 2009.
[23] J. Milewski, K. Świrski, Hybrid – artificial neural network as solid oxide fuel cell model, in: Hydrogen + Fuel Cell, 2009.
[24] Hyprotech Corporation, HYSYS.Plant Steady State Modelling (1998).
[25] J. Milewski, A. Miller, Influences of the type and thickness of electrolyte on solid oxide fuel cell hybrid system performance, Journal of Fuel Cell Science and Technology 3 (4) (2006) 396–402.
[26] Y. Jiang, A. V. Virkar, Fuel composition and diluent effect on gas transport and performance of anode-supported sofcs, Journal of The Electrochemical Society 150 (7) (2003) A942–A951.
[27] F. Zhao, A. Virkar, Dependence of polarization in anode-supported solid oxide fuel cells on various cell parameters, Journal of Power Sources 141 (1) (2005) 79 – 95.
[28] A. Virkar, Theoretical analysis of the role of interfaces in transport through oxygen ion and electron conducting membranes, Journal of Power Sources 147 (1–2) (2005) 8–31.
[29] Łukasz Nikonowicz, J. Milewski, Determination of electronic conductance of solid oxide fuel cells, Journal of Power Technologies 91 (2) (2011) 82–92.
[30] T. Ishihara, T. Shibayama, M. Honda, H. Nishiguchi, Y. Takita, Solid oxide fuel cell using co doped la(sr)ga(mg)o3 perovskite oxide with notably high power density at intermediate temperature, Chemical communications 13 (1999) 1227–1228.
[31] Z. Cai, T. Lan, S. Wang, M. Dokiya, Supported Zr(Sc)O2 SOFCs for reduced temperature prepared by slurry coating and co-firing, Solid State Ionics 152-153 (1) (2002) 583–590.
[32] B. Madsen, S. Barnett, Effect of fuel composition on the performance of ceramic-based solid oxide fuel cell anodes, Solid State Ionics 176 (2005) 2545–2553.
[33] J. Ding, J. Liu, An anode-supported solid oxide fuel cell with spray-coated yttria-stabilized zirconia (ysz) electrolyte film, Solid State Ionics 179 (2008) 1246–1249.
[34] W. Zhou, H. Shi, R. Ran, R. Cai, Z. Shao, W. Jin, Fabrication of an anode-supported yttria-stabilized zirconia thin film for solid-oxide fuel cells via wet powder spraying, Journal of Power Sources 184 (1) (2008) 229–237.
[35] D. Young, A. Sukeshini, R. Cummins, H. Xiao, M. Rottmayer, T. Reitz, Ink-jet printing of electrolyte and anode functional layer for solid oxide fuel cells, Journal of Power Sources 184 (1) (2008) 191–196.
[36] H. Park, A. Virkar, Bimetallic (ni-fe) anode-supported solid oxide fuel cells with gadolinia-doped ceria electrolyte, Journal of Power Sources 186 (2009) 133–137.
[37] Z. Yao, Z. Chunming, R. Ran, R. Cai, Z. Shao, D. Farrusseng, A new symmetric solid oxide fuel cell with La0.8Sr0.2Sc0.2Mn0.8O3-Δ perovskite oxide as both the anode and cathode, Acta Materialia 57 (4) (2009) 1665–1175.
[38] J. Milewski, J. Lewandowski, Comparative analysis of time constants in solid oxide fuel cell processes – selection of key processes for modeling power systems, Journal of Power Technologies 91 (1) (2011) 1–5.
[39] W. Budzianowski, Role of catalytic technologies in combustion of gaseous fuels, Rynek Energii 82 (3) (2009) 59–63.

Nomenclature

δ thickness, μm

$\dot{n}$ molar flow, mol/s

η_f fuel utilization factor

σ conductivity, S/cm

σ_0 factor dependent on material used, S/cm

σ_2 electron conductivity, S/cm

A cell area, cm^2

$E_{\max}$ maximum voltage, V

E_σ factor dependent on material used, J/mol

F Faraday constant, 96,485.3415 C/mol

$i_{\max}$ maximum current density, A/cm^2

p partial pressure, bar

R universal gas constant, 8.315 J/mol/K

r_1 internal ionic area specific resistance, cm^2/S

r_2 internal electron area specific resistance, cm^2/S

T absolute temperature, K